euspen's 21st International Conference & Exhibition, Copenhagen, DK, June 2021
www.euspen.eu

Effect of vibration-assistance on tool wear, process forces and surface roughness when micro milling AISI 316L

Katja Klauer[1], Sebastian Greco[1], Benjamin Kirsch[1], Jan C. Aurich[1]

[1]*Technische Universität Kaiserslautern; Institute for Manufacturing Technology and Production Systems*

katja.klauer@mv.uni-kl.de

Abstract

To improve the process results when micro milling, a unit for vibration-assisted machining was developed. The special characteristic of the unit is that, unlike many commercially available systems, the workpiece itself is excited. With the self-developed vibration unit frequencies up to 15 kHz can be realized and an installation in any machine tool is possible. In general, the process forces and the process results (surface topography of the workpiece) are positively influenced by vibration-assistance when micro milling. Further, a reduction of the process forces usually leads to reduced tool wear. Vibration-assistance hence is especially interesting when micro milling materials where high wear occurs, such as AISI 316L.
The research in this paper focuses on the influence of vibration-assistance on tool wear, process forces and surface roughness during when milling AISI 316L. Single-edged cBN micro milling tools with an effective diameter of 100 µm were used. The vibration excitation of the workpiece led to significant differences in tool wear.

Micro Milling; Vibration-Assistance; AISI 316L; Tool Wear; Process Force

1. Introduction and state of the art

For numerous applications such as electro-mechanical systems or medical devices, increasingly miniaturized and functionalized components are required due to the demand for reduced weight and dimensions [1], which increases the need for highest efficiency and precision when manufacturing structures at micro scale. The structural sizes of such components are usually significantly smaller than 1 mm. One way to produce such features is micro milling [2]. The precision of micro milling processes depends, among other things, on the machine's stiffness [3] and the tool wear [4]. A promising technology to increase precision is vibration-assisted machining, which is already used in macro scale applications. In vibration-assisted machining, the cutting movement of the tool is superimposed with a vibration [5] which leads to changed cutting conditions [6]. In summary, vibration-supported machining is suitable for machining of advanced materials with a high hardness and high wear and temperature resistance [7]. The shorter contact time between tool and workpiece results e.g. in shorter chips and the heat can be dissipated better [8]. Due to the mentioned advantages, vibration-assisted machining is already used for components in aerospace, optics and biomedical science [7].

Vibration-assisted machining was also applied for micro milling [8]. The tool size was 1 mm and titanium and aluminum alloys were machined [8]. The vibration-assisted machining resulted in better surface qualities, quantified by lower *Ra* values. In addition, smaller chips were formed due to the interrupted cut and the process heat was reduced. Noma et al. have observed a reduction of process forces and tool wear when using vibration-assisted machining with tool diameters of d = 400 µm [9]. The vibration direction was in the tool's axial direction, the vibrational frequency was 70 kHz [9]. Different methods exist to realize the excitation. Besides the axial excitation e.g. via the spindle, there is also the excitation via platforms, which are often used for milling applications [7]. Platforms for micro milling are e.g. described in [7-8, 10-13].

In this study the influence of vibration-assistance on the tool wear during micro milling of AISI 316L is investigated. Previous studies by the authors have already shown that micro milling of AISI 316L leads to pronounced abrasive wear [14]. As the focus of this study is the wear behavior of the micro milling tools, AISI 316L is applied. The tools used are single-edged micro end mills with a diameter of d = 100 µm, the direction of the vibration is oriented along the direction of feed motion. Besided the tool wear the process forces during machining and the surface roughness of the milled structures are evaluated.

2. Experimental setup

2.1. Samples and Machine Tool

The material AISI 316L was available as bar material and was cut to the dimensions of 20 x 20 x 7 mm by conventional milling.

The experiments were conducted on the LT Ultra MMC 600 H[a] machine tool. This machine tool features hydrostatic mounted axes and is driven by linear, respectively torque motors (translational axes and rotary axes). Before the study on vibration-assisted micro milling was conducted, the samples were face milled on the UP machine to assure parellism of the sample surface to the tool axes. For this reason, the sample was already fixed to the vibration platform during face milling. A two fluted milling tool with a diameter of 3 mm was used for planning (NS tools MSXH440R[a]).

2.2. Vibration Platform

The design of the vibration platform allows a mounting in different machine tools and is similar to [11-13]. The vibration platform is designed in such a way that it can be screwed onto the dynamometer (Kistler 9119AA2[a]), which is fixed in the machine bed. It consists of a frame, which is fixed on the dynamometer and is also used to preload the piezo, and a workpiece holder (see figure 1a)). The workpiece holder features solid-state joints with a stiffness of approx. 2.2 N/µm. The AISI 316L samples were glued to the workpiece holder. The amplitude of the piezo is calculated according to Melz [15] as follows:

$$\Delta l = \frac{\Delta l_0 \cdot c_{stystem} - F}{c_{system} + c_{piezo}} \quad (1)$$

According to the manufacturer, the piezo (Physik Instrumente, PI) E 618.10G1[a]; max. frequency 15 kHz) has a stiffness of 68 N/µm. This results in a calculated amplitude of 1.8 µm for the construction used.

2.3. Milling Tool and Machining Parameters

Single-edged cBN-tools (NS tools SMEZ120 D0,100[a]) with an effective diameter of d = 100 µm were used for micro milling (see figure 1b). A shrink chuck (Levicron HSW-E[a]) with a static concentricity error < 0.8 µm (manufacturer's specification) was taken for tool clamping. All experiments were performed dry. A microscope was used to observe the micro milling process.

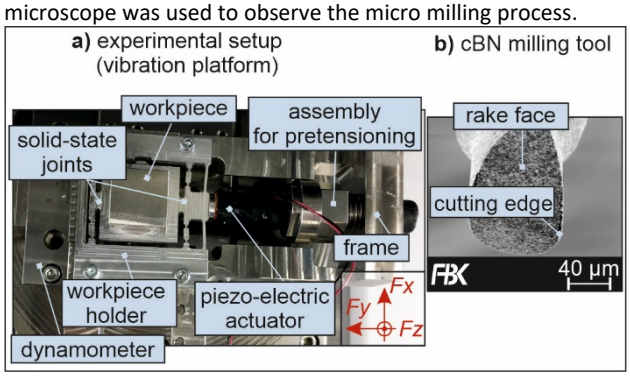

Figure 1. experimental setup: vibration platform and milling tool

The machining parameters are summarized in table 1. The spindle speed was selected as 24,420 rpm, as this avoids a superposition of spindle frequency (f_S = 407 Hz) and vibration-assistance (f_e = 5,130 Hz).

Table 1 machining parameters

parameter	value
spindle speed	24,420 rpm
feed per tooth	1 µm
depth of cut	5 µm
feed travel	340 mm
vibration fequency	5,130 Hz

The vibration frequency was determined as follows: the experimental setup was mounted in the machine tool and the piezo was driven at frequencies ranging from 0 to 20 kHz. The force signal of the dynamometer (offset, without tool engagement) was monitored in real time and the excitation-frequency-dependent maximum of the offset-force was determined. The vibration frequency leading to a maximum in the force signal in direction of the excitation was detected as resonance frequency. For the test setup described, the resonance frequency was 5.13 kHz. The excitation of the sample was performed in the feed direction of the micro milling process. During all tests a feed travel of 340 mm was set. Over the complete feed path the depth of cut was set to 5 µm. This results in a cutting volume of 1,700 mm^2 for a single test. During the test, milling processes without excitation and with excitation in resonance frequency were carried out and the resulting tool wear was compared. The milling processes without excitation served as reference. The tests were performed three times with excitation and without excitation for statistical verification.

3. Measurement Technology

Three different measuring methods were used to detect tool wear and to compare the process results.

3.1. Qualitative wear examination (SEM images)

The tools were sampled with a Philips XL 40[a] scanning electron microscope. For each tool, the entire rake face was sampled.

Before the SEM images were taken, the tools were cleaned in an ultrasonic bath in Isopropanol (5 min). Since all tools were cleaned in the same way, adhering chips indicate changes during the milling process.

3.2. Process Forces

The forces were recorded with the already mentioned dynamometer (Kistler 9119AA2[a]). For all measurements the sampling rate was 12 kHz. The forces were recorded in the following slots:

-slot 1: (0 - 20) mm feed travel
-slot 5: (80 – 100) mm feed travel
-slot 9: (160-180) mm feed travel
-slot 13: (240-260) mm feed travel
-slot 17: (320 – 340) mm feed travel

In the working plane the forces in feed direction (*Fy*) and perpendicular to the feed direction (*Fx*) were measured. Additionally the passive force (*Fz*) was determined. The process force for each slot was determined from the three components (*Fx*, *Fy*, *Fz*) as follows:

- The force components were filtered with a long-wavelength high-pass filter (cut-off frequency 1 Hz), to remove drifts
- When the tool was not engaged, the offset (resulting from: excitation of the workpiece, measuring noise and vibrations) was identified and subtracted from the respective force components
- The total process force was determined from the three components (*Fx*, *Fy*, *Fz*) for each instant of time: the absolute value of the total vector resulting from the vector addition of *Fx*, *Fy* and *Fz* was calculated
- The arithmetic mean value of the process force was determined for each slot
- The specific cutting force was calculated by relating the process force to the actual cutting depth. The cutting depth was determined using images from the confocal microscope (see chapter 4.3).

In addition to the determination in the time domain, the force in feed direction or direction of excitation (*Fy*) was also examined in the frequency domain. Therefore a Fourier analysis of the component *Fy* was performed. By means of this analysis the existing frequencies in the force signal can be identified.

3.3. Surface Roughness

The milled structures were characterized in equal distances (slot 1, 5, 9, 13, 17) with the confocal microscope (Nanofocus µSurf explorer[a]) with an objective that features a 50x magnification and numerical aperture of 0.5. The measuring field size of a single field with this objective is 320 µm x 320 µm. The following two evaluations were performed:

- areal roughness: The suface texture parameter *Sa* (arithmetic mean height) was calculated. One single measuring field was sampled at a position of the slot where the burr does not overhang the structures in the slot's bottom. From this measuring field, an evaluation section of 30 µm x 300 µm was

taken in the middle of the slot. No filtering is prescribed in the standard for the areal surface texture parameters [16]. To eliminate the unavoidable tilting of the sample during the measurement, a plane alignment was performed. In addition, S-filtering with a wavelength of 0.25 µm was performed to remove the measurement noise. For the aligned and filtered section the parameter *Sa* was calculated.

- profile roughness: The profile roughness parameter *Ra* (arithmetic mean height) was determined for the profile in the middle of the slot. To guarantee a profile length of 480 µm, three measuring fields were stichted. The middle profile section was taken from the stitched topography and filtered with λs = 0.25 µm and λc = 8 µm. The filters were defined according to ISO 3274 [17]. Due to the significantly smaller scale of surface roughness and measuring length, the absolute values of the set filters were scaled down.

After the parameters for each individual measured slot were determined as described, they were processed for further consideration as follows: for the two processes (with or without excitation) the parameters of the three repetitions were averaged for the analyzed grooves (1, 5, 9, 13, 17) and the corresponding standard deviations were calculated. In this way, the surface roughness for the two different processes can be shown as a function of the feed travel.

In addition, SEM images of the slots were taken to qualitatively examine the surface quality of the milled slots.

4. Results

4.1. Qualitative wear examination (SEM images)

Figure 2 shows the SEM images of the worn tools after 17 slots corresponding to 340 mm feed travel. When comparing the tools from the tests without excitation and with excitation, it is noticeable that the excitation has an effect on the wear behavior of the tools. However, it is also noticeable that the three tools of the respective tests (with excitation or without excitation) do not show an identical wear. In the upper images for the tests without excitation a considerably wear at the corner is visible. Interestingly, this wear is not always most pronounced at the same position. In repetition 2, the maximum wear of the major cutting edge is slightly higher in the axial direction than for the other two tools. Nevertheless, the wear behavior is basically identical for all three tools: abrasive wear or breakouts occur.

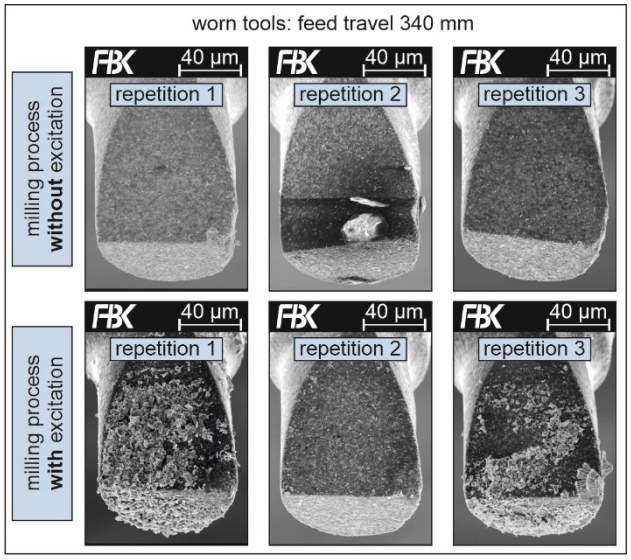

Figure 2. worn tools after 340 mm feed travel

In the experiments with excitation, the wear of the corner appears less pronounced. However, the large number of small chips adhering to the tool during repetition 1 and repetition 3 is striking. A built-up edge has also formed during repetition 3. Since all tools were exposed to the same process conditions (except for the excitation: with or without) and the cleaning strategy was also identical for all tools, it can be assumed that the chip formation was different in the two processes.

4.2. Process Forces

The amplitude spectrum (see figure 3), which was recorded in a milled slot, clearly shows on the spindle frequency with its harmonics and the excitation frequency. The amplitude of the excitation is much more pronounced compared to the spindle's excitation. The frequency of the excitation exceeds the dynamometer's natural frequency (4.6 kHz).

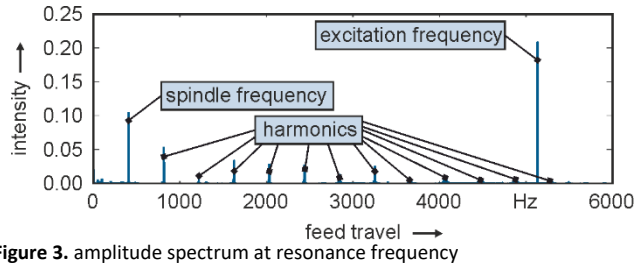

Figure 3. amplitude spectrum at resonance frequency

The specific process forces (mean values) depending on the feed travel are plotted in Figure 4 for all tests. As described in Section 3.2, the mean value of the process force was calculated for each measured slot. It can be seen that all forces are in the same order of magnitude after an initial wear (feed travel > 90 mm). For the tests with excitation, the process forces tend to be almost constant after initial wear.

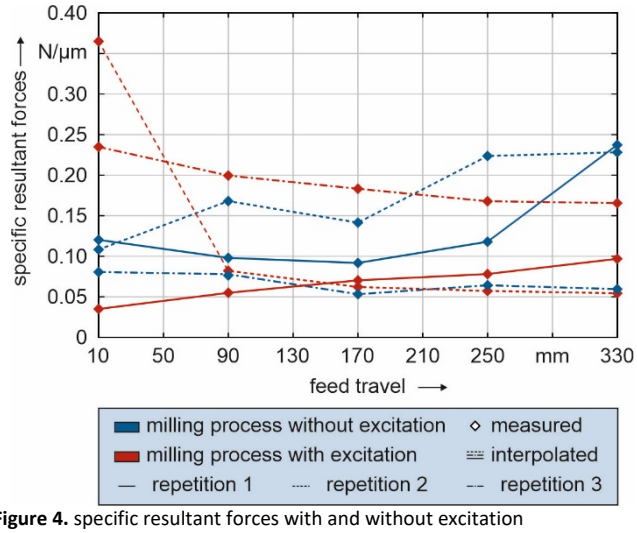

Figure 4. specific resultant forces with and without excitation

4.3. Surface Roughness

For both processes (with and without excitation) the parameter *Sa* shows its maximum value in the first slot. Then (feed travel > 90 mm), the values fluctuate only slightly. *Sa* decreases systematically after the initial wear for the tests with excitation whereas no systematic behavior is visible for the tests without excitation (see figure 5). The values for both processes (with and without excitation) are in an identical order of magnitude.

For *Ra* the behaviour is not systematic and almost constant over all slots and for all conditions. The values for the tests with excitation are always lower than the values for the tests without excitation.

Overall, it can be stated that surface texture and roughness parameters for both processes (with and without excitation) show an almost identical behavior and are of the same order of magnitude. Differences between areal and profile parameters

are mainly due to the fact that only the center profile was considered in the profile analysis and a defined area was examined in the area analysis. The chip thickness decreases during milling with increasing distance from the center axis of the slots. This results in a change in the kinematic roughness as well as increased ploughing effects at the edges of the slots.

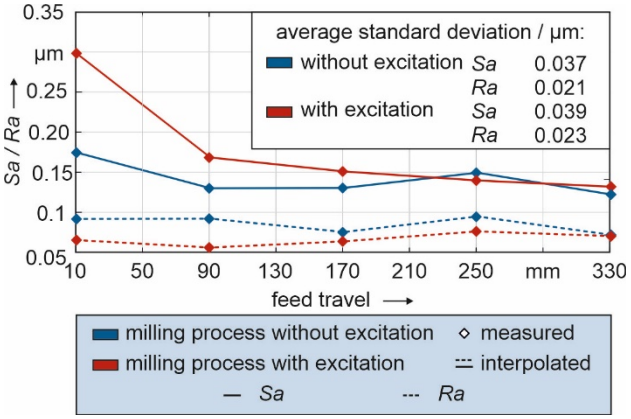

Figure 5. surface texture and roughness parameters with and without excitation

When qualitatively assessing the surface quality in the milled slots on the basis of SEM images, the first thing to note is that there are also differences between the various repetitions within a process (see figure 6).

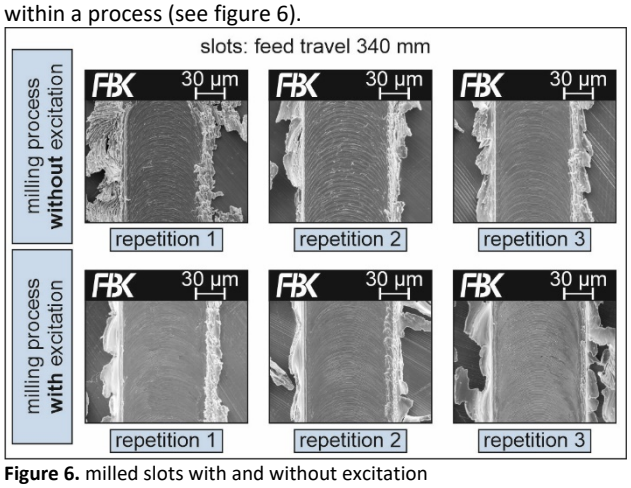

Figure 6. milled slots with and without excitation

However, in the tests without excitation there seems to be a more pronounced tendency for ploughing. This fact may also be due to the abrasive wear which is greater in these tests (see chapter 4.1). Because of the abrasive wear the cutting edge is more rounded and therefore ploughing is more pronounced.

In addition it is visible that the excitation obviously also has an influence on the burr formation. This fact can probably be explained by the changed chip flow, which is caused by the multiple interrupted cut.

5. Conclusion and Outlook

The study examined the influence of vibration-assisted machining on the tool wear and process results in micro milling of AISI 316L. Single-edged cBN milling tools with an effective diameter of 100 µm were used. It was found that the wear on the corner was significantly lower when cutting with excitation. The surface quality of the milled slots with excitation was in the same order of magnitude (*Sa*) or tended to be better (*Ra*) after the initial wear (feed travel > 90 mm). The qualitative assessment of the slot bottom via SEM images showed less smearing of material. This means that the tool life of the micro milling tools can be extended by applying vibration-assistance without deterioration of the surface quality.

Interestingly, there were also differences in burr formation, which were not explicitly investigated in this study. The burr formation will therefore be further investigated in future studies.

[a]Naming of specific manufacturers is done solely for the sake of completeness and does not necessarily imply an endorsement of the named companies nor that the products are necessarily the best for the purpose.

Acknowlegement

The authors would like to thank the German research foundation (DFG) for the financial support within the project AU 185/57-1 “Ultrasonic air bearing spindle for micro machining”. Also funded by the Deutsche Forschungsgemeinschaft (DFG, German Research Foundation) - project number 172116086 - SFB 926.

References

[1] Dornfeld D, Mina S, Takeuchi Y 2006 Recent Advances in Mechanical Micromachining. *CIRP Annals Manufacturing Technology* **55/2** 745-768.

[2] Aurich JC, Reichenbach IG, Schüler GM 2012 Manufacture and application of ultra-small micro end mills. *CIRP Annals Manufacturing Technology* **61/1** 83-86.

[3] Gao X, Li B, Hong J, Guo J 2016 Stiffness modeling of machine tools based on machining space analysis. *International Journal of Advanced Manufacturing Technology* **86/5-8** 2093-2106.

[4] Cheema MS, Dvivedi A, Sharma AK 2015 Tool wear studies in fabrication of microchannels in ultrasonic micromachining. *Ultrasonics* **57** 57-64.

[5] Kumar MN, Subbu SK, Krishna PV, Venugopal A 2014 Vibration Assisted Conventional and Advanced Machining: A Review. *Procedia Engineering* **97** 1577-1586.

[6] Brehl DE, Dow TA 2008 Review of vibration-assisted machining. *Precision Engineering* **32** 153-172.

[7] Yang Z, Zhu L, Zhang G, Ni C, Lin B 2020 Reviwe of ultrasonic vibration-assisted machining in advanced materials. *International Journal of Machine Tools and Manufacture* **156** 103594.

[8] Xu L-H, Na H-B, Han G-C 2018 Machinablity improvement with ultrasonic vibration-assisted micro-milling. *Advances in Mechanical Engineering* **10(12)** 1-2.

[9] Noma K, Takeda Y, Aoyama T, Kakinuma Y, Hamada S 2014 High-Precision and High-Efficiency Micromachining of Chemically Strengthened Glass Using Ultrasonic Vibration. *Procedia CIRP* **14** 389-394.

[10] Ding H, Chen S-J, Cheng K 2011 Dynamic surface generation modeling of two dimensional vibration-assisted micro-end-milling. *International Journal of Advanced Manufacturing Technology* **53** 1075-1079.

[11] Zheng L,. Chen W, Pozzi M, Teng X, Huo D 2019 Modulation of surface wettability by vibration assisted milling. *Precision Engineering* **55** 179-188.

[12] Jin X, Xie B 2015 Experimental study on surface generation in vibration-assisted micro-milling of glass. *Int J Adv Manuf Technol* **81** 507-512.

[13] Chen W, Zheng L, Wenkun X, Yang K, Huo D 2019 Modelling and experimental investigation on textured surface generation in vibration-assisted micro-milling. *Journal of Materials Processing Technology* **266** 339-350.

[14] Greco S, Kieren-Ehses S, Kirsch B, Aurich JC 2020 Micro milling of additively manufactured AISI 316L – Impact of the layerwise microstructure on the process results. . *Int J Adv Manuf Technol* [DOI: 10.1007/s00170-020-06387-3].

[15] Melz T 2001 Entwicklung und Qualifikation modularer Satelitten-Systeme zur adaptiven Vibrationskompensatuon an mechanischen Kryokühlern. Technische Universität Darmstadt.

[16] DIN EN ISO 25178-2 2012: Geometrical product specifications (GPS) – Surface texture: Areal – Part 2: definitions and surface texture parameters.

[17] DIN EN ISO 3274 1998: Geometrical product specifications (GPS) – Surfae texture: Profile method – Nominal characteristics of contact (stylus) instruments.